THE ASTROPHYSICAL JOURNAL, 180: 687–697, 1973 March 15

THE REDSHIFT-DISTANCE RELATION. IV. THE COMPOSITE NATURE OF N GALAXIES, THEIR HUBBLE DIAGRAM, AND THE VALIDITY OF MEASURED REDSHIFTS AS DISTANCE INDICATORS

ALLAN SANDAGE
Hale Observatories, Carnegie Institution of Washington, California Institute of Technology
Received 1972 September 15

ABSTRACT

N galaxies exhibit color and magnitude gradients with changing aperture size that require the presence of two components. A centrally peaked blue source superposed on an extended red component is indicated by new photometry. Calculations by two methods show the central source to have colors of a quasar, and the distended source to have colors and the radial intensity distribution of a giant E galaxy.

N systems are redder than quasars but bluer than normal E galaxies. General considerations require that the intensity ratio of the central mini-quasar to the underlying galaxy is of order unity to explain the color data.

The Hubble diagram for the galaxy component alone in 12 N systems has the same slope, scatter, and zero point as the diagram for radio galaxies, requiring that redshifts of N galaxies have no component, Δz, other than the expansion redshift to within the accuracy of the test. An upper limit on the distribution of Δz can be put as $\sigma(\Delta z/z) \leq 0.1$, and the present data give no evidence that Δz differs from zero.

The Hubble diagram for the companion E galaxies to 3C 303, 3C 371, and 3C 390.3, using the redshifts of their associated N galaxies, leads to the same conclusion. There is no evidence here to support noncosmological redshifts in quasars in view of the absence of such redshifts in N galaxies.

Subject headings: galaxies, photometry of — quasi-stellar sources or objects — redshifts

I. INTRODUCTION

N galaxies, as a class, are intermediate between Seyfert galaxies and quasars in properties of form, color, spectra, redshift, optical and radio variability, and contrast of the central nonthermal component to the total light. Because of this, a sufficiently detailed study of N systems might provide new information on the quasar phenomenon, as regards both the redshift problem and the related question of quasar distances.

Multicolor photometric observations of N systems are presented in this paper. The measurements, made through a series of apertures, generally show a marked reddening and an increase in intensity as the apertures are enlarged (§ II). The spatial distribution of luminosity consists of a centrally condensed blue source with quasar-like colors, and a more widely distributed red component. The relative intensity of the two components and their different spatial distributions can be determined by two separation methods discussed in § III. The Hubble diagram for the galaxy component alone (§ IV), together with other data on redshifts and magnitudes of galaxies that are companions to several N systems, is consistent with the view that N galaxies are at the distance given by their measured redshifts (§ V).

II. OBSERVATIONS

New photometric data were obtained with the prime-focus broad-band photometer at the 200-inch (508-cm) Hale telescope during parts of several observing seasons. Before 1964, an S4 cathode (RCA 1P21) was used: during and after 1967, an S20

(ITT FW130) photomultiplier was used, permitting the measurement of $V - R$ magnitudes. The data were acquired by pulse-counting with equipment built and maintained by the Astroelectronics Laboratory. Companion elliptical galaxies near 3C 303, 3C 371, and 3C 390.3 were also measured.

The new data are listed in table 1, together with most of the single-aperture reconnaissance photometry reported earlier (Sandage 1967*a*, *b*). Tabulated in the various columns are the redshift obtained from sources listed previously (Sandage 1967*a*), with the exception of 3C 303 which is a new value measured from a recent 200-inch Cassegrain Carnegie image-tube spectrogram (five emission lines of λ3727, [Ne III] at λ3869, Hβ, N_1, and N_2); the date of observation; photometer aperture in seconds of arc; and the photometry. The $V - R$ color is on the system of Johnson and Mendoza (JM) rather than on that of Sandage and Smith (1963) because there are more standards available (Iriarte *et al.* 1965; Johnson *et al.* 1966; Mendoza 1967). The primary tie-in was to Mendoza's (1967) data for M67, carried around the sky to a number of secondary standards.[1]

Mean colors from table 1 are plotted in the two-color diagram of figure 1, where the N galaxies are compared with quasars. Quasar data are from the summary catalogue of de Veny, Osborn, and Janes (1971) with the exception that Ton 256 and B264 have been reclassified as N galaxies because of their fuzzy appearance (Arp 1970*a*). The QSO B234 has also been omitted because the intense Hβ, N1, and N2 emission lines at the low redshift give an abnormally bright V-magnitude (Braccesi, Lynds, and Sandage 1968). The N galaxies measured by Westerlund and Wall (1969) are also plotted. No corrections for reddening have been made, either for the quasar or for the N systems. The corrections will be zero above $|b| \geq 50°$ in the reddening model used in Paper II (Sandage 1972*b*), and will be small enough to be neglected for the purposes of the comparison for the other sources.

The marked color separation of quasars and N galaxies is evident. It can be understood as a consequence of differing degrees of contamination of the energy distribution of the underlying galaxy by the blue central source. Clearly, the contamination in N

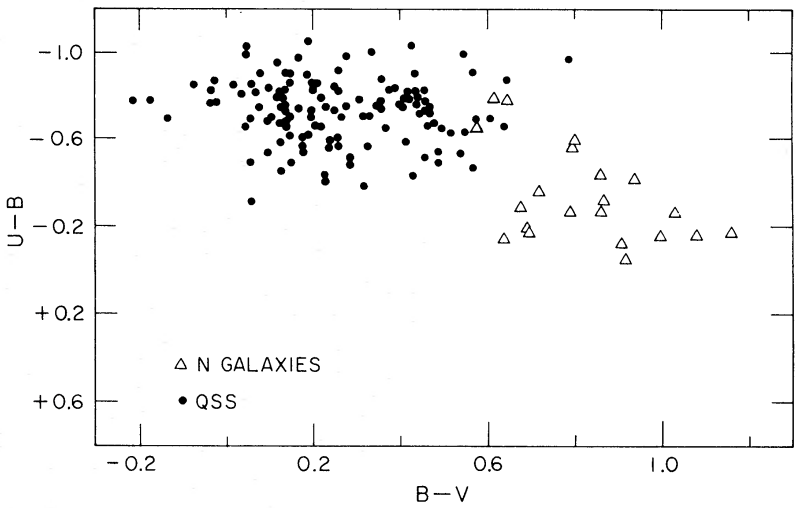

FIG. 1.—The two-color diagram for quasars (*dots*) and N galaxies (*triangles*). No correction for interstellar reddening has been applied. The N galaxy data are taken from table 1 and from photometry by Westerlund and Wall.

[1] The difference between $(V - R)_{JM}$ and $(V - r)_{SS}$ is 6 percent in bandwidth, with a formal transformation of $(V - r)_{SS} = 1.06\ (V - R)_{JM} - 0.04$, determined by a comparison of the *Sky and Telescope* table of Iriarte *et al.* with table 1 of Sandage and Smith.

TABLE 1

PHOTOMETRIC DATA FOR N TYPE RADIO GALAXIES AND COMPANIONS

Object	z	Date	θ	V	B-V	U-B	V-R
3C 79	0.2561	Oct 2/3, 1964	12".19	18.49	0.93	...	...
		Oct 4/5, 1964	12.19	18.62	0.88	...	...
		Sep 10/11, 1967	7.62	18.75	0.79	-0.27	...
		Oct 31/Nov 1, 1967	12.19	18.63	0.78	...	1.50
3C 109	0.3057	Feb 14/15, 1965	12.19	17.76	0.89	-0.08	...
		Sep 10/11, 1967	7.62	18.05	0.93	-0.15	...
		Oct 31/Nov 1, 1967	12.19	18.10	0.87	-0.11	1.45
		Nov 2/3, 1967	7.62	18.02	1.00	...	1.28
		"	12.19	18.01	0.91	-0.29	1.32
		Nov 24/25, 1967	7.62	18.01	0.95	-0.16	1.45
		"	12.19	18.05	0.95	...	1.43
3C 120	0.0333	Sep 10/11, 1967	7.62	14.19	0.46	-0.76	...
		Sep 11/12, 1967	7.62	14.21	0.46	-0.79	...
		"	12.19	14.11	0.49	-0.78	...
		"	18.80	14.02	0.52	-0.75	...
		"	30.59	13.92	0.57	-0.74	...
		Nov 1/2, 1967	7.62	14.23	0.57	-0.78	0.81
		"	12.19	14.14	0.60	-0.75	0.82
		"	18.80	14.07	0.63	-0.74	0.83
		Nov 24/25, 1967	7.62	14.32	0.52	-0.83	0.80
		"	12.19	14.21	0.59	-0.81	0.82
		"	18.80	14.11	0.62	-0.78	0.82
3C 171	0.2384	Oct 2/3, 1964	12.19	18.93	0.95	...	...
		Oct 4/5, 1964	12.19	18.85	0.66	...	...
		Sep 12/13, 1967	7.62	19.08	0.86	0.34	...
		Oct 31/Nov 1, 1967	12.19	18.94	0.49	...	1.25
3C 227	0.0855	Jan 13/14, 1966	12.19	16.44	0.95	-0.39	...
		"	18.80	16.33	0.98	-0.25	...
		Oct 31/Nov 1, 1967	12.19	16.37	0.91	-0.36	0.78
		Apr 29/30, 1971	7.62	16.61	1.06	-0.20	0.94
		"	12.19	16.46	1.06	-0.18	0.96
		"	18.80	16.30	1.02	-0.01	0.89
		"	30.59	16.16	1.08	...	0.86
3C 334	0.1846	May 8/9, 1964	12.19	17.27	0.94	-0.41	
3C 287.1	0.2156	Mar 28/29, 1965	?	18.27	0.92	-0.15	
		Apr 23/24, 1971	12.19	18.02	1.11	-0.14	
3C 303	0.1410	Apr 22/23, 1966	7.62	17.55	1.22	0.03	0.96
		"	12.19	17.25	1.23	0.07	0.97
		"	18.80	17.08	1.22	...	0.95
		June 20/21, 1966	?	17.29	1.08	-0.17	...
3C 303-G1	...	June 28/29, 1971	12.19	17.35	...	...	1.30
		"	18.80	17.11	1.14	...	1.05
3C 303-G3	...	June 28/29, 1971	18.80	17.00	0.76	...	0.78
3C 371	0.0508	Oct 31/Nov 1, 1967	12".19	14.46	0.63	-0.42	0.72
		Nov 2/3, 1967	12.19	14.50	0.65	-0.34	0.72
		Apr 22-24, 1967	4.86	14.94	0.60	-0.41	0.72
			7.62	14.69	0.675	-0.33	0.80
			12.19	14.54	0.69	-0.31	0.80
			18.80	14.44	0.72	-0.28	0.805
			30.59	14.35	0.73	-0.22	0.81
			48.30	14.27	0.76	-0.21	0.77
		Other values for 3C 371 are in Paper II of this series					
3C 371-G1	0.0508	Oct 31/Nov 1, 1967	12.19	16.11	0.99	...	0.86
			18.80	15.88	1.01	...	0.83
		Apr 23/24, 1971	7.62	16.43	1.11	...	...
		"	12.19	16.06	1.09	0.56	...
		"	18.80	15.93	1.03	...	...
3C 390.3	0.0569	Oct 18/19, 1965	7.62	15.49	0.80	-0.59	...
		"	12.19	15.40	0.81	-0.59	...
		Oct 19/20, 1965	12.19	15.38	0.82	-0.56	...
		Sep 8/9, 1967	12.19	15.12	0.67	-0.66	...
		Sep 10/11, 1967	7.62	15.20	0.66	-0.69	...
		"	12.19	15.11	0.68	-0.69	...
		Sep 11/12, 1967	12.19	15.14	0.67	-0.69	...
		Sep 12/13, 1967	12.19	15.10	0.70	-0.62	...
		Oct 27/28, 1967	18.80	14.82	0.53	-0.74	...
		Oct 31/Nov 1, 1967	12.19	14.87	0.57	-0.78	0.76
		Nov 2/3, 1967	12.19	14.90	0.59	-0.74	0.75
		Apr 23/24, 1971	7.62	14.99	0.51	-0.82	0.84
		"	12.19	14.96	0.52	-0.84	0.88
		"	18.80	14.77	0.61	-0.73	0.84
		"	30.59	14.79	0.56	-0.74	0.82
3C 390.3-G1	...	July 11/12, 1964	12.19	16.48	1.16	...	...
		"	18.80	15.98	...	...	...
3C 445	0.0568	July 11/12, 1964	12.19	15.84	1.17	-0.15	...
		"	18.80	15.76	1.15	-0.19	...
		Oct 8/9, 1964	11.39	15.72	1.18	...	...
		"	11.39	15.78	1.20	...	...
		Aug 11/12, 1967	12.19	15.76	1.09	-0.24	...
		Sep 10/11, 1967	7.62	15.86	1.11	-0.22	...
		"	12.19	15.78	1.10	-0.27	...
		Sep 12/13, 1967	12.19	15.81	1.12	-0.31	...
		Oct 31/Nov 1, 1967	12.19	15.76	1.16	-0.23	0.86
		Apr 29/30, 1967	12.19	15.89	1.22	-0.25	0.96
		"	30.59	15.85	...	...	0.87
3C 459	0.2205	July 11/12, 1964	12.19	17.54	0.86	-0.30	...
		Aug 11/12, 1967	7.62	17.59	0.78	-0.35	...
		"	12.19	17.45	0.87	-0.41	...
		Sep 10/11, 1967	7.62	17.62	0.83	-0.36	...
		Oct 31/Nov 1, 1967	7.62	17.58	0.87	-0.29	0.71

systems cannot be large; otherwise the combined light would be dominated by the QSS component, and the composite system would not show the fuzzy envelope (the underlying galaxy) which is the classification characteristic of the N type. Conversely, if the contamination were as small as in Seyfert galaxies, the combined color would be red and the nucleus would be faint. These considerations and model calculations (Sandage 1971) show that N galaxies have intermediate colors and fuzzy outer envelopes because the contamination ratio $a \equiv I(V)_Q/I(V)_G$ is of order unity.

More direct evidence than figure 1 for the existence of an underlying galaxy is contained in table 1 for those sources that were measured with many apertures. If an underlying galaxy is present and has a normal angular diameter for a given redshift (Sandage 1972*a* [hereafter called Paper I], table 1 and figs. 1 and 2), then the ratio of the galaxy light to total light will increase as the aperture size of the photometer is increased. All N galaxies with adequate data in table 1 show this behavior.

It is also required that the colors should redden as the apertures are widened, which they do.

Particularly good examples are 3C 120, where V brightens from 14.21 to 13.92 and the colors redden from $B - V = 0.46$ to 0.57, $U - B = -0.79$ to -0.74, as the aperture diameters increase from 7″.62 to 30″.6; and 3C 371, where V brightens by 0.67 mag and $B - V$ and $U - B$ redden by 0.16 mag and 0.20 mag as θ changes from 4″.9 to 48″.3. The N systems 3C 227, 3C 303, and 3C 390.3 show similar gradients.

Quantitative analysis of the behavior yields intensity and color information on each component separately by methods of the next section.

III. METHODS FOR SEPARATING THE GALAXY AND QSS COMPONENTS

a) The "Galaxy-Growth-Curve-given" Method

Comparison of the normal growth curve for giant E galaxies (e.g., Paper I, table 3) with the slower observed growth in table 1 permits a unique calculation of the contamination ratio I_Q/I_G at the observed wavelength. The higher this ratio, the less effect the distributed galaxy light will have on the total intensity, and the slower will be the observed growth for the composite system.

Before setting out the equations, it is instructive to show directly that the underlying distributed component of 3C 371 has colors of a normal E galaxy. From table 1 consider the 3C 371 data for 1967 April 22–24, where the apertures range from 4″.9 to 48″.3. On the reasonable assumption that the central mini-quasar is unresolved, only light from the extended component will be present in the outer annular zones, even if the seeing disk is as large as 4″. The U, B, V, and R intensities between the 12″.2 and 48″.3 rings give $\Delta U = 0.10$ mag, $\Delta B = 0.20$ mag, $\Delta V = 0.27$ mag, and $\Delta R = 0.24$ mag, which, when normalized to the intensities at the 12″.2 aperture, convert in the standard way[2] to magnitudes for the light in this annulus as $U = 17.46$, $B = 16.96$, $V = 15.91$, and $R = 15.26$. The colors are then $B - V = 1.05$, $U - B = 0.50$, and $V - R = 0.65$, which are normal for a giant elliptical at the redshift of 3C 371.

Consider now the problem of analytically separating the intensities. If large-scale direct plates are available, the diameter of the underlying galaxy θ_s can be measured, and the expected Δ mag $= f(\theta_p)$ found from table 3 of Paper I by normalizing that table to Δ mag $= 0$ at $4.1\theta_s$ which corresponds to the standard metric diameter of $\theta z/(1 + z)^2 = 2.94$. On the other hand, if the diameter θ_s cannot be measured, but if the redshift is known, then table 3 of paper I can be used directly.

[2] The conversion of the light within annulus i, j to magnitude is made by

$$m = 2.5 \log [\text{dex}\,(-0.4m_i) - \text{dex}\,(-0.4m_j)]\,,$$

where m_i is the measured magnitude for light within aperture i. Hence, the U mag for light within radii 12″.2 and 48″.3 is $U = 17.46$ from data in table 1.

Let the measuring apertures be labeled 1, 2, . . . , i, j in order of increasing size. The expected magnitude difference $\Delta m_{i,j}$ between aperture i and j *for a standard galaxy* is assumed to be known via the last paragraph. Denote this difference by $\Delta m(i, j)_{\text{curve}}$. Let the observed difference between apertures i and j be $\Delta m(i, j)_{\text{obs}}$.

The intensity in aperture i is the intensity of the unresolved mini-quasar I_Q, plus the galaxy light within i, denoted by $I_{G,i}$. Similarity with j. Hence,

$$\frac{I_{\text{obs},j}}{I_{\text{obs},i}} \equiv \frac{I_Q + I_{G,j}}{I_Q + I_{G,i}} = \text{dex}\,[0.4\Delta m(i, j)_{\text{obs}}]\,. \tag{1}$$

But

$$I_{G,j}/I_{G,i} = \text{dex}\,[0.4\Delta m(i, j)_{\text{curve}}]\,. \tag{2}$$

Combining equations (1) and (2) with some reduction gives the contamination ratio at aperture i (the smaller) to be

$$a \equiv \frac{I_Q}{I_{G,i}} = \frac{\text{dex}\,[0.4\Delta m(i, j)_{\text{curve}}] - \text{dex}\,[0.4\Delta m(i, j)_{\text{obs}}]}{\text{dex}\,[0.4\Delta m(i, j)_{\text{obs}}] - 1}\,. \tag{3}$$

Once a is known from equation (3), the magnitude difference between the mini-quasar and the galaxy follows as

$$\Delta m_{G,Q} \equiv m_{G,i} - m_Q = 2.5 \log a\,. \tag{4}$$

Let the observed magnitude of the combination at aperture i be $m_{0,i}$, with individual magnitudes $m_{G,i}$ and m_Q. The magnitudes of G_i and Q separately follow from the easily derived equations

$$\begin{aligned} m_{G,i} &= m_{0,i} + 2.5 \log \{1 + \text{dex}\,[0.4(m_{G,i} - m_Q)]\} \\ &= m_{0,i} + 2.5 \log (1 + a)\,, \end{aligned} \tag{5}$$

$$m_Q = m_{G,i} - \Delta m_{G,Q}\,. \tag{6}$$

Knowing $m_{G,i}$ from equation (5) and applying the galaxy growth curve $\Delta m(i, j)_{\text{curve}}$ gives the galaxy magnitude at the standard metric diameter of Paper I (eq. [23]), which solves the problem.

Equations (3)–(6) have been applied to the data for 3C 371 that were obtained on 1967 April 22–24. The results are listed in table 2. The calculated colors for the mini-quasar are $U - B = -0.45$, $B - V = 0.56$, and $V - R = 0.86$, which are similar to those of the quasar 3C 48. The colors of the galaxy are the same as those obtained earlier for the light in the annular ring ($+0.50$, $+1.05$, and $+0.65$).

The galaxy magnitude is $V(48''.3) = 15.15$, and the aperture correction to the standard size is 0.08 mag (Paper I, table 3, with $z = 0.0508$), giving $V_G(\text{std}) = 15.07$. The K_V and A_V corrections are 0.08 and 0.22 mag, respectively, giving $V_C = 14.77$. This magnitude at $z = 0.0508$ puts the galaxy component to 3C 371 at less than 1 σ from the mean line in the Hubble diagram for radio galaxies (Sandage 1972*c*, Paper III). It is well within the scatter of the radio galaxies, which are themselves giant ellipticals. We list in table 2 the observed and the predicted magnitude of the G and Q combination ($m_{0,i}$) on the assumption that m_Q does not vary with aperture. The table was generated by solving equations (3)–(6) for the $12''.19$ aperture only, and assuming that the resulting m_Q was the same for all apertures. Although the run of the predicted minus observed residuals in this table shows that the assumption is not quite correct at the $4''.9$ aperture, we believe this to be an artifact of the observations caused by the effects of seeing at this small aperture rather than caused by a truly extended central source. The general agreement of the observed and predicted growth functions is taken as confirmation of the composite model.

TABLE 2

CONTRIBUTION OF QSS AND GALAXY COMPONENTS FOR 3C 371 AT DIFFERENT APERTURES BY THE "GALAXY-GROWTH-CURVE-GIVEN" METHOD

COLOR	APERTURE					
	4″.86	7″.62	12″.19	18″.80	30″.59	48″.30
U_Q	15.03	15.03	15.03	15.03	15.03	15.03
U_G	18.36	17.80	17.43	17.14	16.87	16.69
U_{obs}	15.13	15.03	14.92	14.88	14.86	14.82
U_{pred}	14.98	14.95	14.92	14.88	14.85	14.82
$P - O$	−0.15	−0.08	0.00	0.00	−0.01	0.00
B_Q	15.48	15.48	15.48	15.48	15.48	15.48
B_G	17.87	17.31	16.94	16.65	16.38	16.20
B_{obs}	15.54	15.36	15.23	15.16	15.08	15.03
B_{pred}	15.37	15.30	15.23	15.16	15.09	15.03
$P - O$	−0.17	−0.06	0.00	0.00	0.01	0.00
V_Q	14.92	14.92	14.92	14.92	14.92	14.92
V_G	16.82	16.26	15.89	15.60	15.33	15.15
V_{obs}	14.94	14.69	14.54	14.44	14.35	14.27
V_{pred}	14.75	14.64	14.54	14.45	14.35	14.27
$P - O$	−0.19	−0.05	0.00	0.01	0.00	0.00
R_Q	14.06	14.06	14.06	14.06	14.06	14.06
R_G	16.16	15.60	15.23	14.94	14.67	14.49
R_{obs}	14.22	13.89	13.74	13.64	13.54	13.50
R_{pred}	13.91	13.82	13.74	13.66	13.57	13.50
$P - O$	−0.31	−0.07	0.00	0.02	0.03	0.00

The principal points to note in table 2 are (1) the dominance of the Q component for the smaller apertures in all colors, (2) the dominance of Q at all apertures in U and B, and (3) the nearly equal contribution of the G and Q component to V at the largest apertures.

Our result for 3C 371 agrees generally with that of Oke (1967) who used a different separation method. As mentioned previously, the Q colors are similar to those of 3C 48, as in Oke's solution. The magnitude of the underlying galaxy over the central 10″ is $V = 16$ here, also as in Oke's solution. It is to be noted that the corrected light of the galaxy to θ_{std} of 64″ is $V_c = 14.77$, which is brighter by 1.2 mag than the value used by Arp (1970*b*) in his discussion of the system.

b) The "Color-given" Method

Growth-curve data as extensive as those for 3C 371 are not available for many N galaxies in table 1, but a method based on color contamination can be used to estimate the contamination ratio.

Let the expected color of the underlying galaxy (corrected for reddening) be $(B - V)_G$, where the effect of redshift is taken into account by adding $K_B - K_V$ to the proper color of a normal giant elliptical. Assume further an unreddened color of $(B - V)_Q$ for the central mini-quasar. Let $(B - V)_{C,i}$ be the observed color of the combination (corrected for reddening) in aperture i.

Aside from a zero point that arises from the definition of the color scales (which cancels out), we have in an obvious notation,

$$I(V)_Q/I(B)_Q = \text{dex}\,[0.4(B - V)_Q]\,, \tag{7}$$

$$I(V)_{G,i}/I(B)_{G,i} = \text{dex}\,[0.4(B - V)_{G,i}]\,, \tag{8}$$

and

$$\frac{I(V)_Q + I(V)_{G,i}}{I(B)_Q + I(B)_{G,i}} = \text{dex}\,[0.4(B - V)_{C,i}]\,. \tag{9}$$

Combining equations (7), (8), and (9) and reducing, gives

$$a_i \equiv \frac{I(V)_Q}{I(V)_{G,i}} = \frac{1 - \text{dex}\,\{0.4[(B - V)_{C,i} - (B - V)_G]\}}{\text{dex}\,\{0.4[(B - V)_{C,i} - (B - V)_Q]\} - 1}\,, \tag{10}$$

which, with equations (4), (5), and (6), solves the problem.[3]

All data in table 1 have been corrected for contamination, using the following steps: (1) Determine $E(B - V)$ for each source in table 1 using equations (2) and (3) of Paper II; (2) find the intrinsic galaxy color from $(B - V)_G = 0.95 + K_B - K_V$, using Whitford's (1971) K-corrections at the observed redshift; (3) assume $(B - V)_Q = 0$, which is the expected mean color of quasars with $z < 0.5$ (cf. Kardashev and Komberg 1966; Barnes 1966; Sandage 1966), and solve for a via equation (10); (4) obtain the individual magnitudes for the quasar and for the galaxy at aperture i using equations (4), (5), and (6); (5) apply the standard galaxy growth-curve to the $V_{G,i}$ values to obtain V_{26}, from which the standard A_V and K_V corrections are subtracted to obtain the corrected galaxy magnitude on the system of Paper III to be used in the Hubble diagram.

The results are listed in table 3 for the particular assumption $(B - V)_Q = 0$. (The relative insensitivity of the result to this assumption is seen in table 3 by comparing the two results for 3C 109, where a second calculation is made by assuming $[B - V]_Q = 0.5$). Listed in column (6) is the derived magnitude of the quasar component; in column (7) is V_{26} for the galaxy (mean of values after aperture correction), and in column (8) is the corrected V-magnitude of the galaxy.

The results of table 3 are consistent with the previous conclusion concerning the

TABLE 3

V-MAGNITUDES FOR THE UNDERLYING GALAXY TO N SYSTEMS CORRECTED FOR APERTURE, K, AND ABSORPTION EFFECTS USING THE "COLOR-GIVEN" METHOD

Object (1)	z (2)	b^{II} (degrees) (3)	K_V (4)	A_V (5)	V_Q (6)	$V_{26,G}$ (7)	$V_{C,G}$ (8)	log cz (9)
3C 79.....	0.2561	−35	0.58	0.14	19.76	18.93	18.21	4.886
3C 109.....	0.3057	−28	0.80	0.23	19.30	18.23	17.20	4.962
3C 109*.....	0.3057	−28	0.80	0.23	18.60	18.76	17.73	4.962
3C 120.....	0.0333	−28	0.05	0.23	14.88	13.92	13.64	4.000
3C 171†.....	0.2384	+22	0.51	0.35	20.16	19.22	18.36	4.854
3C 171†.....	0.2384	+22	0.51	0.00	20.40	19.11	18.60	4.854
3C 227.....	0.0855	+42	0.14	0.07	18.86	16.07	15.86	4.409
3C 234.....	0.1846	+53	0.34	0.00	18.82	17.37	17.03	4.743
3C 287.1.....	0.2156	+63	0.44	0.00	19.83	18.13	17.69	4.811
3C 303.....	0.1410	+58	0.23	0.00	20.04	17.07	16.84	4.626
3C 371.....	0.0508	+29	0.08	0.22	15.78	14.25	13.95	4.183
3C 390.3.....	0.0569	+27	0.09	0.25	15.73	14.91	14.57	4.232
3C 445.....	0.0568	−47	0.09	0.03	> 17	15.02	14.90	4.231
3C 459.....	0.2205	−51	0.46	0.00	18.85	17.67	17.21	4.820

* Second entry for 3C 109 calculated with $(B - V)_Q = 0.5$.

† For 3C 171, two cases assumed as $A_V = 0.35$ and $A_V = 0$ based on $E(B - V) = 0.13$ and 0.0.

[3] The a defined here is the contamination ratio in the observer's V passband. It differs from the ratio defined in the earlier discussion (Sandage 1971, tables 4 and 5) because it was taken there to be the ratio at the proper wavelength in the galaxy frame. The present definition is more convenient for use in the actual observations.

TABLE 4

COLORS AT VARIOUS CONTAMINATION RATIOS AND REDSHIFTS*

Mix		$z = 0.00$		$z = 0.10$		$z = 0.20$	
a	$V_G - V_C$	$B - V$	$U - B$	$B - V$	$U - B$	$B - V$	$U - B$
0.0....	0.00	0.95	+0.62	1.30	+0.43	1.59	+0.22
0.1....	0.10	0.82	+0.16	1.09	−0.03	1.30	−0.20
0.2....	0.20	0.72	−0.06	0.95	−0.23	1.11	−0.37
0.3....	0.28	0.65	−0.20	0.84	−0.35	0.97	−0.47
0.5....	0.44	0.53	−0.36	0.68	−0.48	0.78	−0.57
1.0....	0.75	0.37	−0.54	0.47	−0.61	0.53	−0.67
1.5....	0.99	0.29	−0.61	0.36	−0.67	0.40	−0.71
2.0....	1.19	0.23	−0.65	0.26	−0.70	0.32	−0.73
∞.....	∞	0.00	−0.80	0.00	−0.80	0.00	−0.80

* Underlying quasar component assumed to have intrinsic colors of $B - V = 0.00$, $U - B = -0.80$. Galaxy assumed to have colors $(B - V) = 0.95$, $U - B = 0.62$ of a normal giant elliptical at $z = 0$.

contamination ratio. Light from the central mini-quasar does not overwhelm the galaxy component as it does in QSSs.

It is instructive to trace the locus of the changing color contamination in the $(U - B, B - V)$ diagram as a is increased. An elaborate solution was previously made using numerical integrations discussed elsewhere (Sandage 1971), but the same qualitative results can be obtained analytically. As the ratio a is varied, it can be shown that $(B - V)_C$ and $(U - B)_C$ of the mix are given by

$$(B - V)_C = (B - V)_Q + 2.5 \log \left\{ \frac{1 + a^{-1}}{1 + \text{dex}\,[0.4(B_Q - B_G)]} \right\}, \tag{11}$$

$$(U - B)_C = (U - B)_Q + 2.5 \log \left\{ \frac{1 + \text{dex}\,[0.4(B_Q - B_G)]}{1 + \text{dex}\,[0.4(U_Q - U_G)]} \right\}, \tag{12}$$

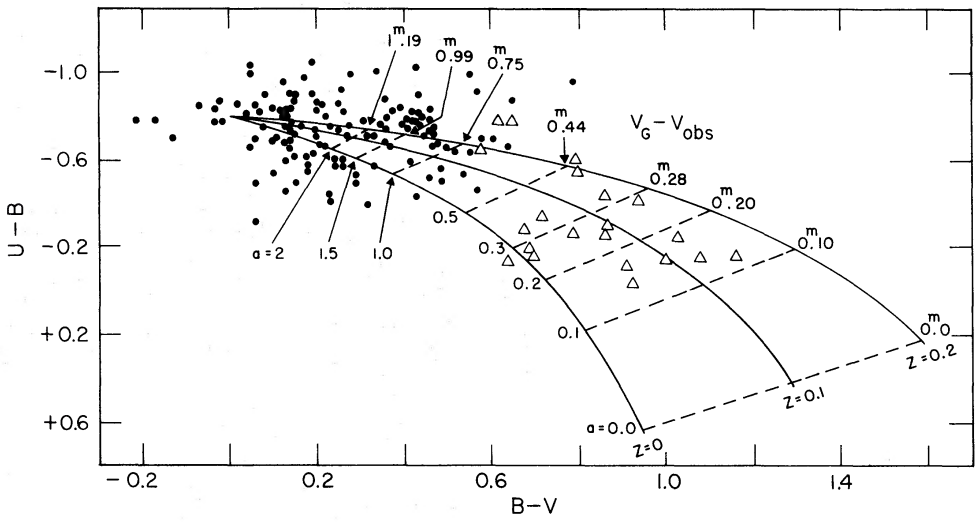

FIG. 2.—Same as fig. 1 but with loci of the color variation of a composite N system as the contamination ratio is varied from 0 to ∞ for redshifts of $z = 0.0$, 0.1, and 0.2. The components of the mix consist of an E galaxy of intrinsic color $(B - V)_G = 0.95$ and $U - B = 0.62$ at $z = 0$, and an unresolved central nonthermal source of $(B - V)_Q = 0.0$, $(U - B)_Q = -0.8$. Data for the lines are from table 4.

where

$$B_Q - B_G \equiv (B - V)_Q - (B - V)_G - 2.5 \log a\,, \tag{13}$$

and

$$U_Q - U_G \equiv (U - V)_Q - (U - V)_G - 2.5 \log a\,. \tag{14}$$

The color loci as functions of a and z found from these equations are listed in table 4 and are plotted in figure 2 for three redshift values. The observations are the same as in figure 1. The contamination values, a, are shown along the lower $z = 0$ boundary. The corresponding magnitude difference $m_G - m_C$ between the galaxy and the composite system from equation (5) is shown along the upper ($z = 0.2$) curve.

From this diagram it is clear why N galaxies are those systems where a is generally less than 1, as betrayed by their red $B - V$ colors and their moderate to large ultraviolet excess.

Are the redshifts of N galaxies due solely to the expansion?

IV. THE HUBBLE DIAGRAM

The V_C galaxy magnitudes in column (8) of table 3 are plotted against redshift in the Hubble diagram of figure 3. For comparison, radio galaxies taken from Paper III (table 2, cols. [6] and [11]) are shown as dots.

The close agreement of the triangles and the dots is the central result of this paper. Although it is to be emphasized that the contamination corrections of table 3 are formal because the colors of the central mini-quasar are assumed by the "color-given" method, the data of table 3 (col. [8]) cannot be changed by more than $\pm \sim 0.5$ mag for any reasonable variation in these colors [i.e., $\Delta(B - V) \simeq \pm 0.5$ mag]. Nor are the differences between the two separation methods significant relative to the total spread of the dots in figure 3.

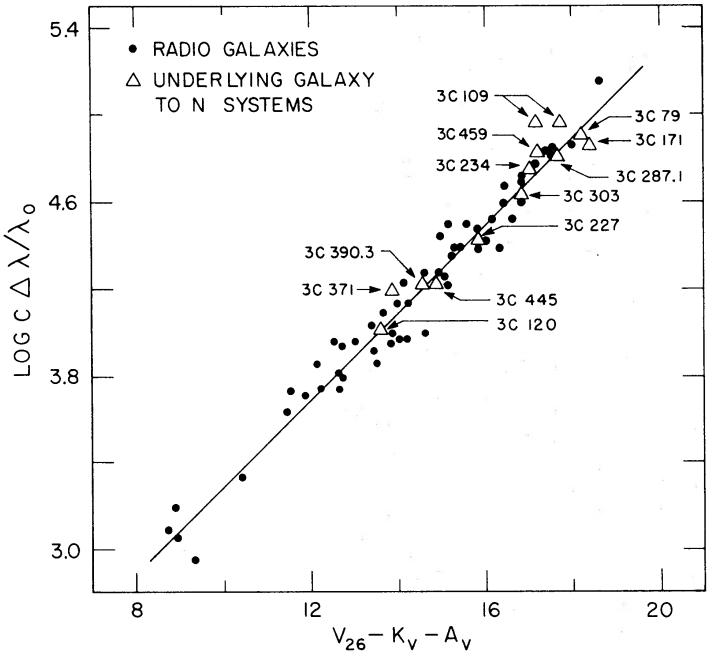

FIG. 3.—The Hubble diagram for the underlying galaxy component of N systems (*triangles*), compared with the radio galaxies listed in Paper III. The galaxy magnitudes are corrected for aperture, K, and absorption effects. Redshifts are the measured values for the nonthermal N components. Data for the triangles are from table 3.

TABLE 5

APERTURE CORRECTIONS FOR COMPANION GALAXIES TO 3C 303, 3C 371, AND 3C 390.3

Object	ΔX	ΔY	z	θ	$\log \theta z/(1+z)^2$	ΔV	V_{obs}	V_{26}	V_c	$\log z$
(1)	(2)	(3)	(4)	(5)	(6)	(7)	(8)	(9)	(10)	(11)
3C 303−G1....	134″E	39″N	0.1410	12″19	+0.121	−0.29	17.35	17.06		
				18.80	+0.309	−0.12	17.11	16.99		
								17.03	16.80	4.626
3C 303−G3....	214 E	102 S	0.1410	18.80	+0.309	−0.12	17.00	16.88		
								16.88	16.65	4.626
3C 371−G1....	52 W	64 S	0.0508	7.62	−0.455	−1.20	16.43	15.23		
				12.19	−0.251	−0.82	16.08	15.26		
				18.80	−0.063	−0.53	15.90	15.37		
								15.29	14.99	4.183
3C 390.3−G1	200 E	240 N	0.0569	12.19	−0.207	−0.74	16.48	15.74		
				18.80	−0.019	−0.46	15.98	15.52		
								15.63	15.29	4.232

The principal conclusion is that the agreement of the N data with a line of slope of 5, and the agreement of zero points between the distribution of triangles and dots, leave no margin for extraneous redshift effects Δz superposed on the expansion redshifts of N galaxies. The tightness of fit of the triangles to the line gives an upper limit on sigma of the distribution of $\Delta z/z$ as $\sigma(\Delta z/z) \lesssim 0.1$. There is no evidence from the data themselves that Δz is other than zero when the distribution of horizontal residuals for radio galaxies (e.g., $\sigma[\Delta M_V] = 0.48$ mag from fig. 3 of Paper III) is taken into account.

The same conclusion follows from data on galaxies in groups associated with the N systems. Among others, the sources 3C 234, 3C 303, 3C 371, and 3C 390.3 in the present sample are associated with companion E galaxies. Photometry for galaxies in the last three groups is set out in table 1, and is shown in more detail in table 5. The galaxies can be identified from the ΔX and ΔY coordinates in columns (2) and (3), measured from the N galaxy.

Details of the aperture correction are given in columns (5), (6), and (7), where the Δ mag $= f(z, \theta_p)$ method of Paper I was used. Because the systems in question are similar to the first-ranked member in magnitude, the use of this method will not significantly overestimate the intensity (V_{26}) because the difference between the true diameter and that assumed will be $\Delta \log \theta \lesssim 0.1$, which, by § V*a* of Paper I, gives an error of less than 0.1 mag in V_{26}.

The agreement of the several V_{26} values in column (9) of table 5, especially for 3C 371−G1, shows that these companion galaxies have radial intensity distributions that are similar to that of the giant E galaxies used for the growth curve of Paper I. From this, and from the observed colors in table 1, the companions are clearly normal E galaxies in their radial intensity distribution $I(r)$.

The V_C values from table 5 (col. [10]), plotted in figure 3 using the redshift of the companion N galaxy, are within the scatter of the other plotted points.[4] This is taken as additional evidence that the redshift values are those expected from the expansion

[4] The photometric data for the 3C 371 group and the conclusions therefrom differ from those of Arp (1970*b*) because his estimated magnitude of 3C 371−G1 was $V = 17$, rather than $V = 15$. For 3C 371 itself, he used $V_C = 16$ rather than $V_C = 14.77$ derived here.

alone. Further confirmation is available from Arp's (1970*b*) observations that the redshift of 3C 371 – G1 is the same as that of 3C 371 itself.

V. CONCLUSIONS

The magnitude and color gradients in table 1 show that giant elliptical galaxies form the dominant component of N systems. Separation of the galaxy and the mini-quasar contributions in 12 N systems shows that the mean absolute magnitude of the underlying galaxy is the same as for radio galaxies, as given by the Hubble diagram.

If the intensity of the nonthermal blue source in N galaxies were to be turned higher, the composite color would become bluer (fig. 2), and the object would be called a quasar. If quasars are, in fact, maxi-N galaxies, they must, on this model, appear to the left of the radio galaxy line in the Hubble diagram, as indeed they do (Paper III, fig. 4).

The redshifts of N galaxies have no detectable noncosmological component. The evidence that such systems are at their Hubble distance consists of (1) the normality of figure 3, (2) the compatibility of the angular diameters of the underlying galaxy with the θ, z relation for giant ellipticals (Paper I) as inferred from the smallness of the $P - O$ residuals in table 2 where the method of separation relies on the validity of the adopted growth curve, (3) the equality of the measured redshifts of 3C 371 and its normal E companion, and (4) the fit of 3C 303 – G1 and 3C 390.1 – G1 to the line in figure 3.

Because the classification of N galaxies and quasars depends on the presence or absence of a fuzzy outer envelope, and because detection of this envelope depends on such extraneous factors as (1) the focal length and f ratio of the telescope, (2) the distance of the object, and (3) the contamination ratio a, there is no evidence via this route through N galaxies to attribute noncosmological redshifts to quasars in view of the absence of such redshifts in N galaxies.

It is a pleasure to thank Juan Carrasco and Gary Tuton, night assistants at the 200-inch, for their cheerful help in obtaining the observations, and the personnel of the Astroelectronics Laboratory for providing the equipment, maintenance, and electronic set ups. It is also a particular pleasure to acknowledge the gift of computing equipment by Francis Moseley with which the analysis of the data was made.

REFERENCES

Arp, H. C. 1970*a*, *Ap. J.*, **162**, 811.
———. 1970*b*, *Ap. Letters*, **5**, 75.
Barnes, R. 1966, *Ap. J.*, **146**, 285.
Braccesi, A., Lynds, R., and Sandage, A. 1968, *Ap. J.* (*Letters*), **152**, L105.
de Veny, J. B., Osborn, W. H., and Janes, K. 1971, *Pub. A.S.P.*, **83**, 611.
Iriarte, B., Johnson, H. L., Mitchell, R. I., and Wisniewski, W. Z. 1965, *Sky and Tel.*, **30**, 21.
Johnson, H. L., Mitchell, R. I., Iriarte, B., and Wisniewski, W. Z. 1966, *Comm. Lunar and Planetary Lab.*, **4**, No. 63.
Kardashev, N. S., and Komberg, B. V. 1966, *Astr. Circ. USSR*, No. 357.
Mendoza, E. E. 1967, *Bol. Obs. Tonantzintla y Tacubaya*, **4**, No. 29.
Oke, J. B. 1967, *Ap. J.* (*Letters*), **150**, L5.
Sandage, A. 1966, *Ap. J.*, **146**, 13.
———. 1967*a*, *Ap. J.* (*Letters*), **150**, L9.
———. 1967*b*, *ibid.*, p. L177.
———. 1971, *Optical Properties of Nuclei*, in *Semaine d'Etude sur Les Noyaux des Galaxies*, Pont. Acad. Sci. Scripta Varia, No. 35, ed. D. O'Connell, p. 271.
———. 1972*a*, *Ap. J.*, **173**, 485 (Paper I).
———. 1972*b*, *ibid.*, **178**, 1 (Paper II).
———. 1972*c*, *ibid.*, p. 25 (Paper III).
Sandage, A., and Smith, L. L. 1963, *Ap. J.*, **137**, 1057.
Westerlund, B. E., and Wall, J. V. 1969, *Ap. J.*, **74**, 335.
Whitford, A. E. 1971, *Ap. J.*, **169**, 215.